J Interv Card Electrophysiol (2013) 36:233–242
DOI 10.1007/s10840-012-9733-y

Rapid acquisition of high-resolution electroanatomical maps using a novel multielectrode mapping system

Leon M. Ptaszek · Fadi Chalhoub · Francesco Perna · Roy Beinart · Conor D. Barrett · Stephan B. Danik · E. Kevin Heist · Jeremy N. Ruskin · Moussa Mansour

Received: 31 May 2012 / Accepted: 14 September 2012 / Published online: 22 November 2012

Abstract
Purpose Conventional electroanatomical mapping systems employ roving catheters with one or a small number of electrodes. Maps acquired using these systems usually contain a small number of points and take a long time to acquire. Use of a multielectrode catheter could facilitate rapid acquisition of higher-resolution maps through simultaneous collection of data from multiple points in space; however, a large multielectrode array could potentially limit catheter maneuverability. The purpose of this study was to test the feasibility of using a novel, multielectrode catheter to map the right atrium and the left ventricle.
Methods Electroanatomical mapping of the right atrium and the left ventricle during both sinus and paced rhythm were performed in five swine using a conventional mapping catheter and a novel, multielectrode catheter.
Results Average map acquisition times for the multielectrode catheter (with continuous data collection) ranged from 5.2 to 9.5 min. These maps contained an average of 2,753 to 3,566 points. Manual data collection with the multielectrode catheter was less rapid (average map completion in 11.4 to 18.1 min with an average of 870 to 1,038 points per map), but the conventional catheter was slower still (average map completion in 28.6 to 32.2 min with an average 120 to 148 points per map).
Conclusions Use of this multielectrode catheter is feasible for mapping the left ventricle as well as the right atrium. The multielectrode catheter facilitates acquisition of electroanatomical data more rapidly than a conventional mapping catheter. This results in shorter map acquisition times and higher-density electroanatomical maps in these chambers.

L. M. Ptaszek · F. Chalhoub · F. Perna · R. Beinart · C. D. Barrett · S. B. Danik · E. K. Heist · J. N. Ruskin · M. Mansour (✉)
MGH Heart Center, Cardiac Arrhythmia Service,
Massachusetts General Hospital,
55 Fruit Street, GRB-109, Boston, MA 02114, USA
e-mail: mmansour@partners.org

Keywords Animal studies · Biomedical engineering · Electroanatomical mapping · Catheter ablation

1 Introduction

The technology for electroanatomical mapping of cardiac chambers was first introduced in the 1990s [1–3]. This mapping technology, which has since become an essential tool for the ablation of cardiac arrhythmias, is based on simultaneous recording of spatial information and electrical activity from electrodes placed on a roving catheter. Maps generated with these systems are highly accurate and facilitate localization and ablation of arrhythmias [2, 4–10]. This mapping technology is now in widespread use for arrhythmia ablation worldwide [11–13] and has facilitated improvements in understanding of the anatomic substrate of some arrhythmias [14, 15].

With the conventional form of this mapping system, electrical activation data are gathered using a single or a small number of electrodes on a roving catheter. Map acquisition can be labor intensive and time consuming. Obtaining electrical conduction maps of intermittent phenomena, such as ectopic beats, can be particularly challenging. Collection of electroanatomical data from a large number of electrodes simultaneously could potentially accelerate the rate at which data are collected, leading to creation of more detailed maps in a shorter period of time. Rapid rate of point collection may also increase the likelihood that comparatively rare events are captured in a facile manner.

Initial efforts to place multiple electrodes on a single mapping catheter were limited by electrode size. Electrode technology has since improved, and it is now possible to place multiple electrodes on a catheter whose tip is the same diameter as a standard mapping/ablation catheter. Several multielectrode catheters with varying configurations have been described [15–19]. These multielectrode mapping catheters facilitate the creation of high-density electroanatomical maps

through simultaneous collection of data from closely spaced electrodes. The extra detail provided by high-density maps is thought to be particularly useful in the ablation of challenging arrhythmias, such as atrial tachycardia after ablation for atrial fibrillation [15, 20]. The detailed maps produced by multielectrode catheters have also been utilized to decrease the amount of fluoroscopy use during ablation procedures [21].

A novel, multielectrode catheter and its integrated mapping system (Rhythmia Medical, Burlington, MA), were recently tested in a canine model [22]. In this animal model, it was demonstrated that the multielectrode catheter was capable of producing high-resolution electroanatomical maps of the right atrium. The electrodes at the tip of this catheter are arranged in a spherical array, which is larger than the tip of a conventional mapping catheter (Fig. 1). The size of this array raised concerns regarding the maneuverability of the catheter in other cardiac chambers, particularly the left ventricle. The purpose of the experiments described in this report was to determine the feasibility of using this novel, multielectrode catheter to create electroanatomical maps of the left ventricle in addition to the right atrium. The performance of the multielectrode catheter (speed of point acquisition and point density in completed maps) was compared in these two chambers. The performance of the multielectrode catheter in these chambers was also compared with that of a conventional, single-electrode mapping catheter.

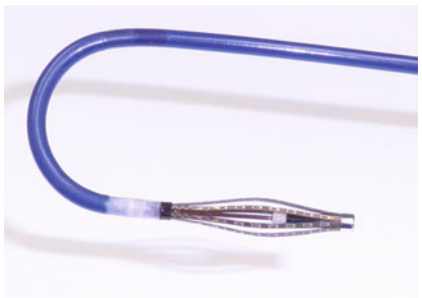

Undeployed

Deployed

Fig. 1 Pictures of the multielectrode catheter in both undeployed and deployed positions. Multiple electrodes are arranged in longitudinal arrays on eight splines. These splines flex when the catheter tip is mechanically deployed, producing a spherical shape that maximizes the number of electrodes in contact with a chamber wall

2 Methods

2.1 Multielectrode catheter and integrated mapping system

The multielectrode mapping catheter has an 8 Fr profile and is equipped with a mechanism for bidirectional tip deflection. At the catheter tip, there are 64 electrodes distributed on eight splines (Fig. 1). The interelectrode spacing is 2.5 mm, and each electrode has a surface area of 0.4 mm^2. The electrode array can be deployed into a spherical configuration through mechanical flexion of the splines. Deployment is controlled from the catheter handle and variable levels of deployment (3–22 mm) can be achieved. Electrodes were used in bipolar and unipolar configurations. A flushing mechanism is present at the catheter tip to prevent thrombus formation.

The multielectrode catheter evaluated in this study is part of an integrated electroanatomical mapping system, which also includes an electronic patient interface unit and a computer workstation that is used to run the mapping software. The position of the multielectrode array is tracked with a combination of magnetic and electrical field information. There is a magnetic sensor near the catheter tip, and impedance is measured through each individual electrode. With this system, an electrical conduction map and an anatomical shell can be constructed simultaneously.

2.2 Integration of cardiac beats into an electroanatomical map

An individual cardiac beat detected by the catheter is added to the map only when the following criteria are satisfied: the collecting electrode remains in a stable point in space, timing of the sensed electrogram (EGM) is stable with respect to a reference EGM (timing is measured using the point of maximum amplitude of the bipolar signal or the maximum negative dV/dt of the unipolar signal), the cycle length of the cardiac rhythm is stable, and the beat is detected within the selected respiratory gate (the respiratory cycle is tracked by measuring impedance change across the chest). The parameters for these criteria are set by the operator before mapping is begun (e.g., measurement of cardiac cycle length and definition of respiratory gate).

2.3 Construction of an electroanatomical shell

The anatomical shell is constructed by aggregating all electrode locations associated with accepted beats. The locations of the outermost electrodes thus define the endocardial surface of a chamber. EGMs acquired in the context of accepted beats were incorporated into the electrical conduction map only if the collecting electrode was within 3 mm from the constructed endocardial boundary. The fill radius applied to the constructed anatomical shell around each

collected point was 2 mm for the multielectrode catheter and 7 mm for the conventional catheter. Completeness of each map was determined empirically by the operator. A map was considered complete when all anatomical landmarks (e.g., right atrial appendage, inferior vena cava, superior vena cava, and aortic valve annulus) were visible.

2.4 Data acquisition modes

Two acquisition modes are available with the multielectrode catheter: continuous and manual. In the continuous data acquisition mode, operator-defined criteria for accepting cardiac beats (described in Section 2.2) are applied during map construction without immediate input from the operator. The EGMs from collected beats are annotated by the system. In the continuous point collection mode, the map can therefore be created by uninterrupted movement of the catheter. In the manual data acquisition mode, the operator collects data in an "area-by-area" manner. The operator moves the catheter to an area of space, reviews the acceptance criteria, and then manually decides whether or not the position is to be incorporated into the map. The EGM is also annotated manually. With the conventional mapping catheter, only manual point collection was performed.

2.5 Map editing

Removal of inaccurate data is possible after data acquisition is complete. Possible revisions include removal of anatomic points and re-annotation of EGMs. Maps created with either continuous or manual point collection can be revised; however, post-acquisition editing was considered to be particularly important for maps constructed using the continuous point collection method since editing of data is not performed by the operator during acquisition. Editing involved moving the catheter to revisit all areas of the existing map. The software allowed for visualization of the EGM associated with each anatomic point, which facilitated re-annotation. The decisions to remove beats and re-annotate EGMs were made by the operator. In this study, maps collected in manual mode were not edited.

2.6 Experimental protocol

Experiments were conducted with five adult swine weighing between 35 and 45 kg. This study protocol was reviewed and approved by the Subcommittee for Research Animal Care at the Massachusetts General Hospital, according to the American Association of Laboratory Animal Care standards for proper research animal care. After overnight fasting, the animals were brought to the procedure suite, general anesthesia was induced, and vital signs were monitored continuously.

2.7 Catheter setup

In all cases, a 5 Fr steerable decapolar catheter (St. Jude Medical, St. Paul, MN) was placed in the coronary sinus via the jugular vein. This catheter was used for recording of atrial EGMs and atrial pacing. The right atrium and the left ventricle were mapped using two catheters: the conventional single-electrode catheter and the multielectrode catheter. Mapping catheters were advanced to the right atrium from the femoral vein and to the left ventricle via the femoral artery.

2.8 Anatomical reconstruction and activation mapping

Maps of the cardiac chambers constructed with the multielectrode catheter were compared with maps constructed with the conventional catheter. In each animal studied, the right atrium and the left ventricle were mapped repeatedly with both catheters during sinus rhythm and paced rhythm. Catheters were therefore handed to the operator in random order to minimize the potentially confounding effect of operator knowledge of the chamber being mapped. Right atrial mapping in paced rhythm was performed with the same catheter setup as was used in sinus rhythm. Pacing was performed from the distal dipole of the coronary sinus catheter. Mapping of the left ventricle in paced rhythm required an additional pacing catheter, which was inserted in the epicardial space and placed adjacent to the inferolateral wall.

2.9 Collection and comparison of mapping process data

The time required to generate each map was recorded, as was the number of points collected. These data are listed in Figs. 5 and 6 and in Table 1. Maps constructed with continuous point collection were edited after point acquisition was completed. The amount of required post-acquisition editing and the total time required to complete the editing were recorded. Corresponding data are listed in Table 2.

2.10 Statistical analysis

The paired *t* test was used to compare the following measurements: total map acquisition time, total points collected per map and points collected per minute during map acquisition. The two-tailed test was performed, because it was not assumed that the multielectrode catheter was superior. This test was used in all instances where matched pairs could be compared. For left ventricular mapping in the context of epicardial ventricular pacing, matched pairs were not available for all comparisons: four animals were mapped using the conventional catheter and five animals were mapped

Table 1 Atrial and ventricular map construction using the multielectrode catheter and its integrated mapping system

Rhythm	Catheter type (acquisition mode)	Number	Map acquisition time in min(mean ± SD)		Total points acquired per map (mean ± SD)	
Right Atrium						
Sinus rhythm	Multi-electrode (continuous)	5	5.6 ± 1	P = .0049	2,753 ± 365	P < .0001
	Multi-electrode (manual)	5	11.4 ± 5.5	P = .0042	878 ± 219	P < .0001
	Conventional (manual)	5	28.6 ± 9.5	P = .0018	124 ± 53	P = .001
Atrial pacing	Multi-electrode (continuous)	5	5.2 ± 0.8	P = .015	3,566 ± 1,082	P = .0037
	Multi-electrode (manual)	5	14.3 ± 5.4	P = .012	979 ± 179	P = .002
	Conventional (manual)	5	31.1 + 13.2	P = .023	148 ± 76	P = .00027
Left Ventricle						
Sinus rhythm	Multi-electrode (continuous)	5	9.5 ± 1.4	P = .00019	3,379 ± 1,156	P = .011
	Multi-electrode (manual)	5	18.1 ± 2	P = .00068	1,038 ± 232	P = .0029
	Conventional (manual)	5	32.2 ± 6.2	P = .0024	135 ± 66	P = .00055
Epicardial pacing	Multi-electrode (continuous)	5	7.1 ± 2.1	P = .002	2,833 ± 738	P = .002
	Multi-electrode (manual)	5	13.1 ± 2.2	P < .0001	870 ± 203	P < .0001
	Conventional (manual)	4	30.7 ± 12.3	P = .0003	120 ± 45	P < .0001

using the two multielectrode catheter-based methods. Therefore, the Generalized Estimating Equations approach (SAS PROC GENMOD) with identity mean link function was used in this instance [23].

3 Results

Maps of the right atrium and the left ventricle were generated with the multielectrode and conventional catheters in

Table 2 Map revision required after continuous data collection using the multielectrode catheter

Chamber	Rhythm	Number	Accepted beats per map (mean±SD)	Manually overridden beats per map (mean±SD)	% manually overridden beats per map (mean±SD)	Manually re-annotated EGMs per map (mean±SD)	% manually re-annotated EGMs (per map (mean±SD)
Right atrium	Sinus rhythm	5	275±55	5±3	1.7±0.6	8±3	0.3±0.1
	Paced rhythm	5	324±98	4±3	1.4±1.4	8±9	0.2±0.3
Left ventricle	Sinus rhythm	5	474±118	3±4	0.6±0.9	2±3	0.1±0.1
	Paced rhythm	5	329±81	4±1	1.1±0.4	4±4	0.1±0.1

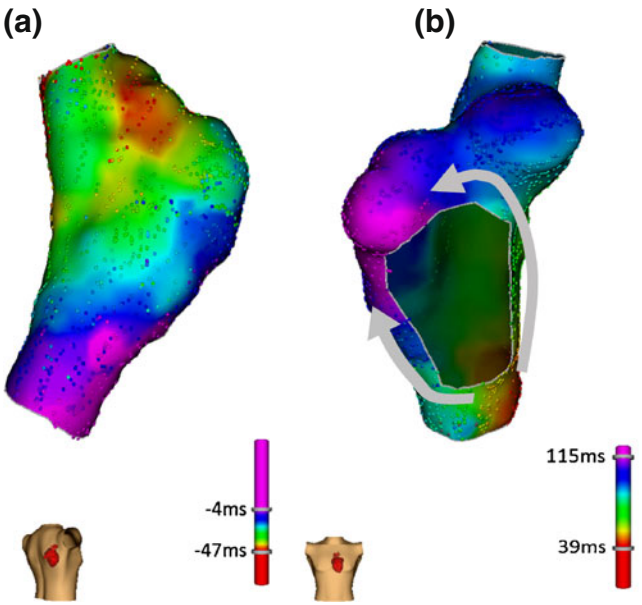

Fig. 2 Right atrial maps generated with the novel multielectrode catheter. *Dots on the maps* represent the points at which electrode contact led to anatomic and EGM data acquisition. Reference for activation timing is present on the *right-hand side of each image*. The picture of the human torso present at the *left-hand side of each image* serves as an additional indicator of the map view. (**a**) Right posterior oblique (*RPO*) view of the right atrial map generated in the context of sinus rhythm. The site of earliest activation is shown in *red* and is visible near the expected position of the sinus node, at the junction between the atrium and superior vena cava. (**b**) Anteroposterior (*AP*) view of the right atrial map generated in the context of atrial pacing from the distal coronary sinus. The tricuspid annulus is visible en face. The site of earliest activation, again shown in *red*, is visible in the interatrial septum. This site is distinct from the noted location of the sinoatrial node. *Arrows* indicate direction of wavefront propagation around the tricuspid annulus

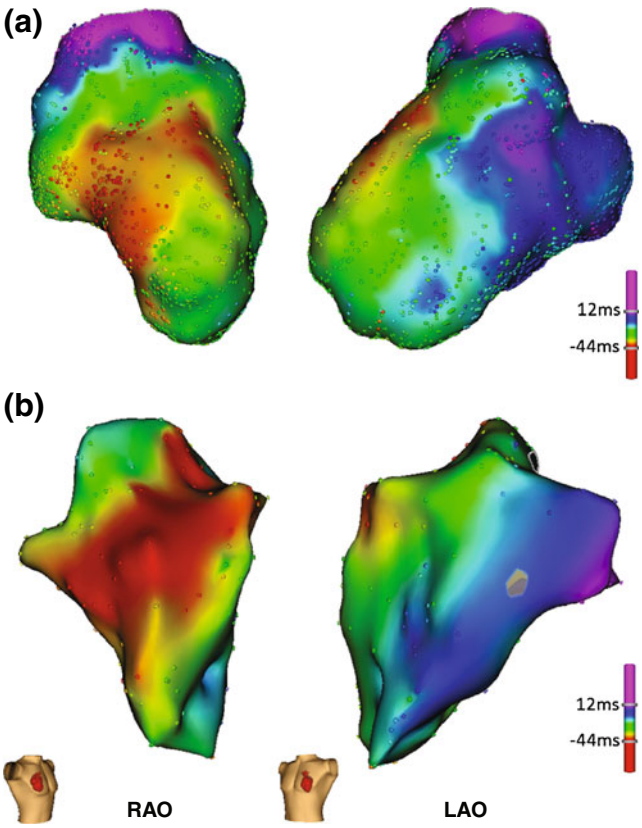

Fig. 3 Comparison of left ventricular maps generated with the multielectrode and conventional catheters in normal sinus rhythm. *Dots on the maps* represent the points at which electrode contact led to anatomic and EGM data acquisition. Reference for activation timing is present on the *right-hand side of each panel*. This timing applies to both views in each panel. (**a**) Right anterior oblique (*RAO*) and left anterior oblique (*LAO*) views of the left ventricular map generated using the multielectrode catheter, with continuous point collection. The site of earliest activation, shown in *red*, is visible in the expected position in the interventricular septum. (**b**) RAO and LAO views of the left ventricular map generated with the conventional mapping catheter. Activation map generated using the conventional catheter is superimposed on the electroanatomical shell generated with the multielectrode catheter. The site of earliest activation, again shown in *red*, is visible in the interventricular septum

the context of both sinus rhythm and paced rhythm (Figs. 2, 3, and 4). Comparison of map acquisition times revealed that electroanatomical data collection with the multielectrode catheter was faster than with the conventional catheter (Table 1; Figs. 5 and 6). All observed differences in catheter performance were statistically significant with $P<0.05$.

In sinus rhythm, construction of right atrial maps with the multielectrode catheter in continuous data collection mode took an average of 5.6 min. Manual data collection with the multielectrode catheter was associated with a longer average completion time of 11.4 min. Irrespective of point collection mode, map construction with the multielectrode catheter was significantly shorter than with the conventional catheter (average map completion time 28.6 min). The multielectrode catheter also produced the shortest map construction times for the left ventricle in sinus rhythm. Average map completion times in this context were: 9.5 (multielectrode catheter with continuous point collection), 18.1 (multielectrode catheter with manual point collection), and 32.2 min (conventional catheter). In the context of paced rhythm, the multielectrode catheter again produced quicker map completion times than the conventional catheter in both chambers. As was observed in sinus rhythm, continuous point collection with the multielectrode catheter was faster than manual point collection (Table 1; Figs. 5 and 6).

Even in the context of shorter map completion times, the multielectrode catheter produced maps with higher point density than the conventional catheter. In sinus rhythm, right atrial maps constructed with the multielectrode catheter in continuous point collection mode contained an average of 2,753 points. Use of manual data collection

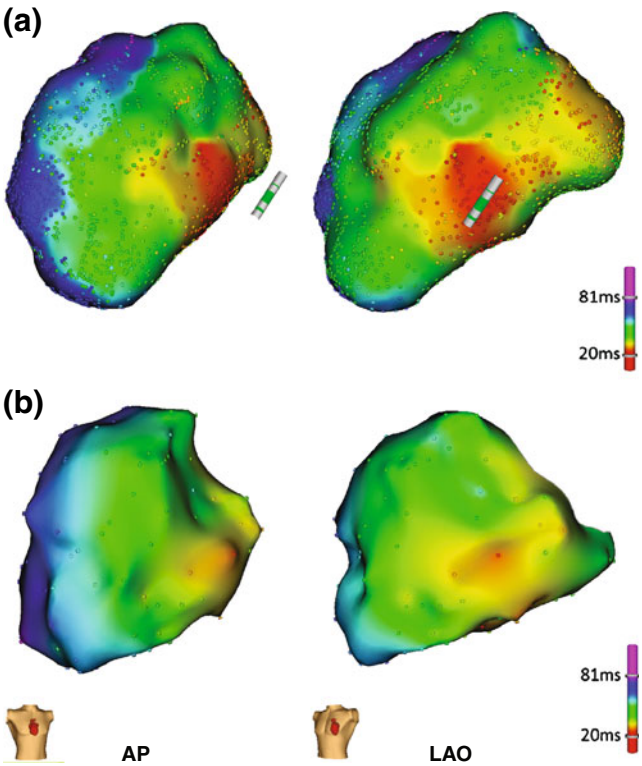

Fig. 4 Comparison of left ventricular maps generated with the multielectrode and conventional catheters during ventricular pacing. *Dots on the maps* represent the points at which electrode contact led to anatomic and EGM data acquisition. Reference for activation timing is present on the *right-hand side of each panel*. This timing applies to both views in each panel. (**a**) AP and LAO views of the left ventricular map generated using the multielectrode catheter, with continuous point collection. The site of earliest activation, shown in *red*, is visible on the inferior wall. This site is directly adjacent to the site of the tip of the pacing catheter, whose location is displayed. (**b**) AP and LAO views of the left ventricular map generated using the conventional mapping catheter. Activation map generated using the conventional catheter is superimposed on the electroanatomical shell generated with the multielectrode catheter. The site of earliest activation, again shown in *red*, is visible on the inferior wall

with this catheter resulted in lower average point density (878 points), which was still significantly higher than the point density produced with the conventional catheter (124 points). A similar trend was observed in the ventricle. Maps produced with the multielectrode catheter in continuous data collection mode contained an average of 3,379 points. In manual data collection mode, the average number of points per map was 1,038. The conventional catheter was associated with the lowest average point density (135 points per map). The multielectrode catheter also produced maps with higher point density in the context of paced rhythm (Table 1).

The amount of post-acquisition editing required for maps constructed with the multielectrode catheter using continuous point collection was measured in order to determine the extent to which editing would offset the speed of point acquisition in this mode (Table 2). Two types of editing were performed: (1) removal of beats in the context of poor catheter contact and (2) re-annotation of EGMs. For each map, the total number of overridden beats was calculated, as was the total number of EGMs requiring re-annotation. The total numbers of overridden beats and re-annotated EGMs per map were small. The average number of beats acquired per map of the right atrium in sinus rhythm was 275. Of the acquired beats, an average of 5 (1.7 %) were manually overridden. An average of eight EGMs were re-annotated per atrial map in sinus rhythm, representing 0.3 % of the average 2,753 EGMs collected per map. Maps of the left ventricle acquired in sinus rhythm required a comparable degree of revision: 474 beats were acquired per map and 3 beats (0.6 %) were manually overridden, on average. Of the 3,379 EGMs collected on average for each ventricular map in sinus rhythm, re-annotation was performed for an average of 2 (0.1 %). In the context of paced rhythm, revision requirements were similar (Table 2). Visual inspection of the maps after editing did not reveal any significant changes in conduction sequence or in the anatomic shell (data not shown).

Editing took a maximum of 2 min to complete for atrial maps and a maximum of 3.1 min to complete for ventricular maps. Since very few alterations in the map were made, the length of the editing process was driven largely by the time taken by the operator to revisit all areas in the constructed map with the catheter. In order to determine whether or not post-acquisition editing would offset the speed advantage of continuous point collection, the total map procedure time (mean map acquisition time plus maximum editing time) in continuous mode was compared with map acquisition time in manual mode. The maximum editing time was used in order to provide a conservative estimate of the impact of editing. It was found that the total map procedure time for continuous mode was significantly shorter than manual map acquisition in most, but not all, cases. Total map procedure time for the left ventricle in sinus rhythm was 12.54±1.4 min in continuous mode, versus 18.1±1 min in manual mode (P=0.001). For left ventricular mapping in paced rhythm, total map procedure time was 10.14±2.1 min in continuous mode versus 13.1±2.2 min in manual mode (P=0.03). For right atrial mapping in sinus rhythm, total map procedure time for continuous mode was not significantly shorter than for manual mode: 7.54±1 versus 11.4±5.5 min, P=0.14. Total map completion time for the right atrium in paced rhythm was 7.42±0.8 min in continuous mode versus 14.3±5.4 min in manual mode (P=0.04).

4 Discussion

4.1 Map generation with the multielectrode catheter system

In this preclinical study, we tested a novel, multielectrode catheter and its associated mapping system. The primary findings of this study are the following. Anatomical and activation mapping with the multielectrode catheter system were feasible in the left ventricle as well as in the right atrium. Maps were acquired more rapidly with the multielectrode catheter than with the conventional mapping catheter in both chambers. The point density of maps produced with the multielectrode catheter was far higher than the density achieved with the conventional mapping catheter (Table 1; Figs. 5 and 6). The increase in point density achieved with the multielectrode catheter in the left ventricle was comparable to the increase achieved in the right atrium. Mapping with the multielectrode catheter was performed in two different modes of point acquisition: continuous and manual. Maps produced using the continuous mode contained a markedly higher point density than maps produced using the manual mode. Mean map acquisition time was shorter in the continuous mode than in the manual mode in all cases. When post-acquisition editing was taken into account, this statistically significant reduction in procedure time was observed in most, but not all, cases. Very few changes were made during editing. Although visual comparison of the conduction sequences and anatomic shells of unedited and edited maps did not reveal significant differences (data not shown), further analyses will be required to assess whether or not maps generated with continuous point collection may be used without editing. It was therefore concluded that performance of the multielectrode catheter, as measured by speed of data acquisition and point density, was comparable in the right atrium and the left ventricle.

The importance of electroanatomical mapping technology has increased as a result of the growth in the number of electrophysiologic procedures requiring detailed knowledge of cardiac anatomy and activation [7, 8, 12–14, 17, 24–26]. Electroanatomical mapping facilitates acquisition of detailed information regarding cardiac anatomy with spatial localization error of <1 mm [7, 11, 13, 17, 26–28]. This technology has been used to pinpoint the electrophysiologic substrate of

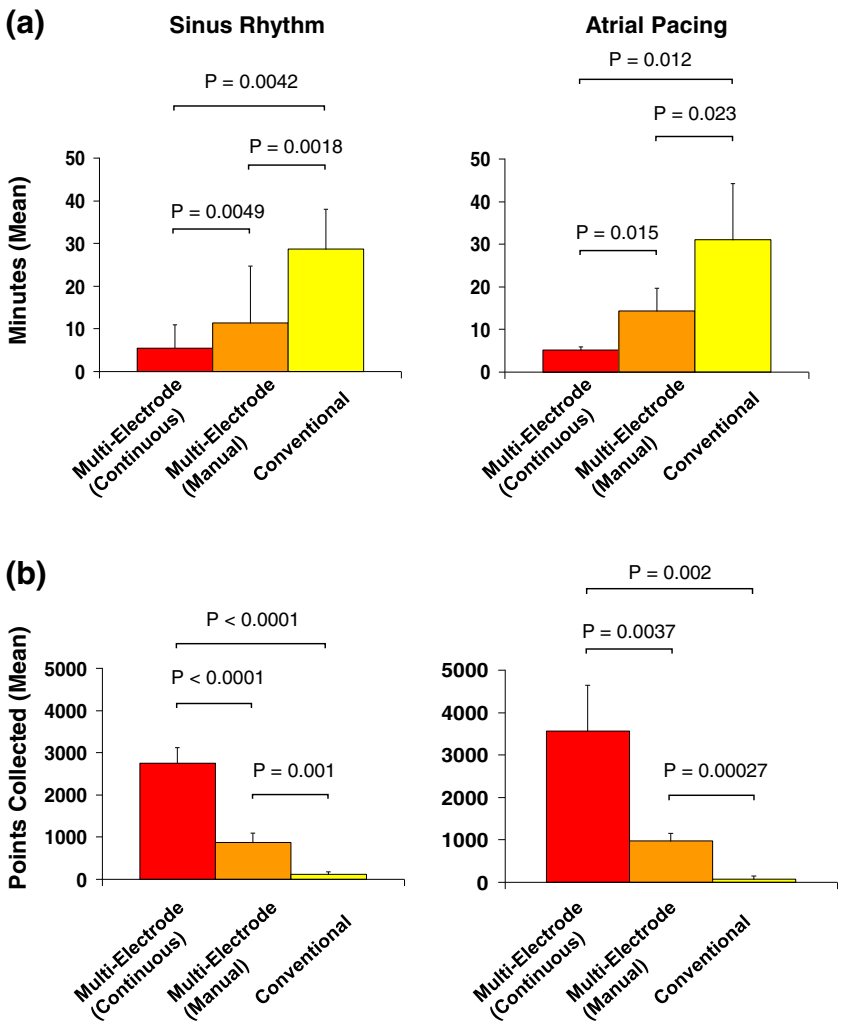

Fig. 5 Right atrial mapping: comparison of multielectrode and conventional catheter performance. (**a**) Map acquisition time in the context of normal sinus rhythm and atrial pacing from the distal coronary sinus. Mean values are reported in the bar graph, and the *error bars* correspond to one standard deviation. Acquisition time is shortest for the multielectrode catheter with continuous point collection in both sinus and paced rhythm. Slowest map acquisition time is for the conventional catheter, with an intermediate map acquisition time noted for the multielectrode catheter with manual acquisition. (**b**) Number of points collected in each map in the context of normal sinus rhythm and atrial pacing from the distal coronary sinus. Mean values are reported in the bar graph, and the *error bars* correspond to one standard deviation. The number of points acquired per map is greatest for the multielectrode catheter with continuous point collection in both sinus and paced rhythm. The smallest number of points per map was acquired with the conventional catheter

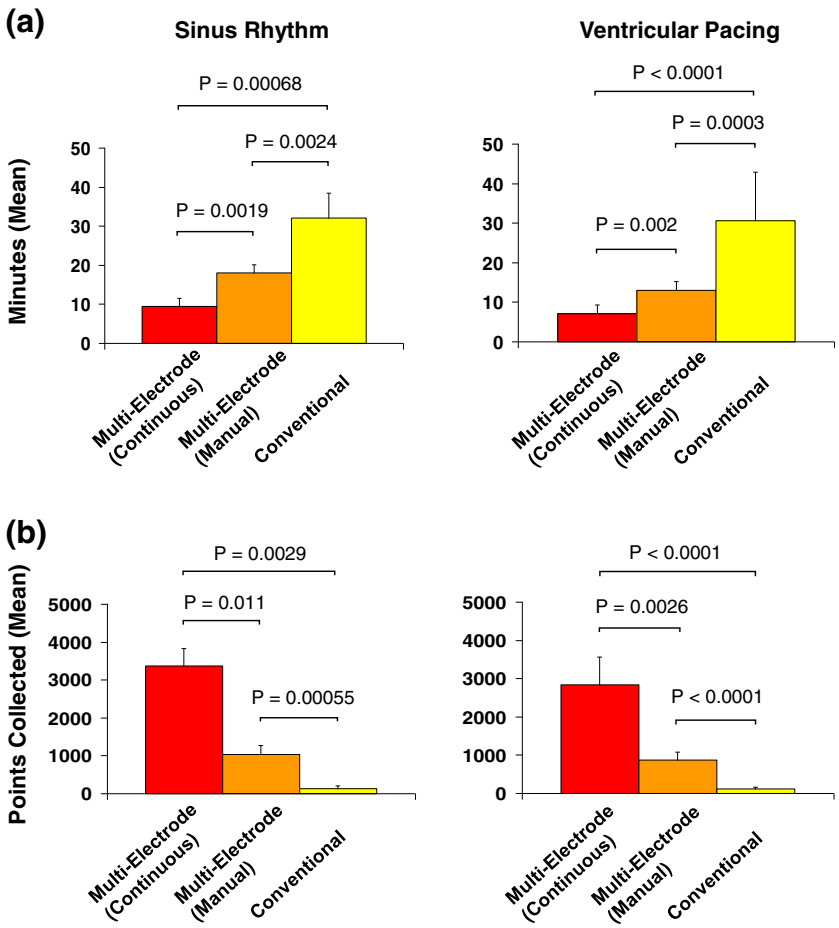

Fig. 6 Left ventricular mapping: comparison of multielectrode and conventional catheter performance. (**a**) Map acquisition time in the context of normal sinus rhythm and ventricular pacing from the epicardial surface. Mean values are reported in the bar graph, and the *error bars* correspond to one standard deviation. Acquisition time is shortest for the multielectrode catheter with continuous point collection in both sinus and paced rhythm. Slowest map acquisition time is for the conventional catheter. (**b**) Number of points collected in each map in the context of normal sinus rhythm and ventricular pacing from the epicardial surface. Mean values are reported in the bar graph, and the *error bars* correspond to one standard deviation. The number of points acquired per map is greatest for the multielectrode catheter with continuous point collection in both sinus and paced rhythm. Smallest number of points per map was acquired with the conventional catheter

multiple arrhythmias [7–14] and to guide endomyocardial biopsies [28, 29]. Use of this system with a conventional mapping catheter has several drawbacks, notably the time-consuming nature of sequential, "point-by-point" map acquisition. This limitation led to the innovation of several multielectrode mapping catheter systems, which facilitate rapid collection of high-density maps through simultaneous collection of data from multiple points in space. Noncontact mapping provides multiple, simultaneous virtual EGMs of the mapped chamber [19]. This system can facilitate the mapping of non-sustained arrhythmias from as little as one beat by giving a global impression of activation sequence; however, the virtual unipolar EGMs are susceptible to error at the boundaries of the mapping field. A multispline catheter has been used to produce high-density atrial maps (through direct mapping) that identify the source of atrial tachycardias and complex fractionated EGMs [17, 20]. This catheter has been used for electroanatomical mapping using impedance-based [15, 30] and magnetic localization systems [18].

The multielectrode catheter described in this study, which contains a higher number of electrodes than previously described multispline catheters [15, 17, 18, 20], is no less maneuverable than a conventional mapping catheter in the left ventricle and right atrium. The multielectrode catheter produced complete maps of the right atrium and left ventricle, and there were no anatomic areas in either chamber that could be mapped more effectively with the conventional catheter. Gross pathological analysis of the left ventricle and right atrium after mapping did not reveal any evidence of catheter-related injury.

4.2 Limitations

The testing described in this study involved a limited number of iterations, possibly reducing the statistical power of the analyses. Mapping was performed in stable rhythms, so the performance of the system in mapping complex arrhythmias and detecting rare phenomena was not tested. This study was designed to test the feasibility of using the multielectrode catheter for mapping of the left ventricle. All testing was performed on animals with normal hearts, and further testing will be required to assess the performance of the system with myocardial scar. Only the right atrium and left ventricle were tested, so performance of the multielectrode catheter system in the right ventricle and left atrium is not addressed here. The multielectrode catheter described in this study is compatible only with its matched mapping system. Since this mapping system is compatible only with

the described multielectrode catheter and the conventional mapping catheter, comparisons of different multielectrode catheters were not possible.

5 Conclusions

Electroanatomical mapping using this novel, multielectrode catheter has been shown to facilitate construction of right atrial maps that are more detailed than is routinely possible using a conventional mapping catheter. Due to the size of the multielectrode array, there was concern that this catheter may not be sufficiently maneuverable in the left ventricle to allow for effective mapping. The results of this preclinical study suggest that use of this multielectrode catheter for electroanatomical mapping of the left ventricle is feasible. Every area of the left ventricle that was accessible with the conventional mapping catheter was also accessible with the multielectrode catheter. There was no gross pathological evidence of injury induced by the multielectrode catheter. The multielectrode catheter produced higher density maps of the left ventricle than the conventional mapping catheter. Total mapping time of the left ventricle with the multielectrode catheter was shorter than with the conventional catheter. Comparable increases in left ventricular map density and decreases in map acquisition time associated with the multielectrode catheter were observed in the right atrium. This novel catheter may therefore facilitate mapping of arrhythmias in the left ventricle as well as the right atrium.

Acknowledgments L.M.P. received research support from the Deane Institute for Integrative Research Atrial Fibrillation and Stroke at the Massachusetts General Hospital. Statistical analyses were performed with support from Harvard Catalyst/The Harvard Clinical and Translational Science Center (NIH award No. UL1 RR 025758 and financial contributions from Harvard University and its affiliated academic health care centers).

Financial disclosures Leon M. Ptaszek, M.D., Ph.D., Fadi Chalhoub, M.D., Francesco Perna, M.D., Roy Beinart, M.D., Conor D. Barrett, M.D., and Stephan B. Danik, M.D. have no financial disclosures to declare. E.Kevin Heist, M.D., Ph.D. declares no financial support but with potential conflicts of interest from the following: Boston Scientific (research grant and honoraria), Biotronik (research grant and honoraria), Boston Scientific (research grant, consultant, and honoraria), Medtronic (honoraria), Sanofi (consultant), Sorin (consultant and honoraria), and St. Jude Medical (research grant, consultant, and honoraria). Jeremy N. Ruskin, M.D. declares no financial support but with potential conflicts of interest from the following: Atricure (consultant), Biosense Webster (consultant and fellowship support), Boston Scientific (fellowship support), CardioFocus (Clinical Oversight Committee—no compensation), CardioInsight (Scientific Advisory Board), CryoCath (Scientific Steering Committee—no compensation), Medtronic (consultant and fellowship support), St. Jude Medical (fellowship support), and Third Rock Ventures (consultant). Moussa Mansour, M.D. declares the following disclosures: Biosense Webster (consultant and research grant), Boston Scientific (consultant and research grant), St. Jude Medical (consultant and research grant), Medtronic (consultant), MC 10 (research grant), Voyage Medical (research grant), Rhythmia Medical (research grant), and CardioFocus (research grant).

References

1. Ben-Haim, S. A., Osadchy, D., Schuster, I., Gepstein, L., Hayam, G., & Josephson, M. E. (1996). Nonfluoroscopic, *in vivo* navigation and mapping technology. *Nature Medicine, 2*, 1393–1395.
2. Shpun, S., Gepstein, L., & Ben-Haim, S. A. (1997). Guidance of radiofrequency endocardial ablation with real-time three-dimensional magnetic navigation system. *Circulation, 96*, 2016–2021.
3. Gepstein, L., Hayam, G., & Ben-Haim, S. A. (1997). A novel method for nonfluoroscopic catheter-based electroanatomical mapping of the heart: *in vitro* and *in vivo* accuracy results. *Circulation, 95*, 1611–1622.
4. Gepstein, L., & Evans, S. J. (1998). Electroanatomical mapping of the heart: basic concepts and implications for the treatment of cardiac arrhythmias. *Pacing and Clinical Electrophysiology, 21*, 1268–1278.
5. Smeets, J. L., Ben-Haim, S. A., Rodriguez, L. M., Timmermans, C., & Wellens, H. J. (1998). New method for nonfluoroscopic endocardial mapping in humans: accuracy assessment and first clinical results. *Circulation, 97*, 2426–2432.
6. Gepstein, L., Wolf, T., Hayam, G., & Ben-Haim, S. A. (2001). Accurate linear radiofrequency lesions guided by a nonfluoroscopic electroanatomic mapping method during atrial fibrillation. *Pacing and Clinical Electrophysiology, 24*, 1672–1678.
7. Boulos, M., & Gepstein, L. (2004). Electroanatomical mapping and radiofrequency ablation of an accessory pathway associated with a large aneurysm of the coronary sinus. *Europace, 6*, 608–612.
8. Boulos, M., Lashevsky, I., & Gepstein, L. (2005). Usefulness of electroanatomical mapping to differentiate between right ventricular outflow tract tachycardia and arrhythmogenic right ventricular dysplasia. *The American Journal of Cardiology, 95*, 935–940.
9. Corrado, D., Basso, C., Leoni, L., Tokajuk, B., Bauce, B., Frigo, G., et al. (2005). Three-dimensional electroanatomic voltage mapping increases accuracy of diagnosing arrhythmogenic right ventricular cardiomyopathy/dysplasia. *Circulation, 111*, 3042–3050.
10. Corrado, D., Basso, C., Leoni, L., Tokajuk, B., Turrini, P., Bauce, B., et al. (2008). Three-dimensional electroanatomical voltage mapping and histologic evaluation of myocardial substrate in right ventricular outflow tract tachycardia. *Journal of the American College of Cardiology, 51*, 731–739.
11. Packer, D. L. (2005). Three-dimensional mapping in interventional electrophysiology: techniques and technology. *Journal of Cardiovascular Electrophysiology, 16*, 1110–1116.
12. Nademanee, K., McKenzie, J., Kosar, E., Schwab, M., Sunsaneewitayakul, B., Vasavakul, T., et al. (2004). A new approach for catheter ablation of atrial fibrillation: mapping of the electrophysiologic substrate. *Journal of the American College of Cardiology, 43*, 2044–2053.
13. Koa-Wing, M., Ho, S. Y., Kojodjojo, P., Peters, N. S., Davies, D. W., & Kanagaratnam, P. (2007). Radiofrequency ablation of infarct scar-related ventricular tachycardia: correlation of electroanatomical data with post-mortem histology. *Journal of Cardiovascular Electrophysiology, 18*, 1330–1333.
14. Marchlinski, F., Zado, E., Dixit, S., Gerstenfeld, E., Callans, D., Hsia, H., et al. (2004). Electroanatomic substrate and outcome of catheter ablative therapy for ventricular tachycardia in setting of right ventricular cardiomyopathy. *Circulation, 110*, 2293–2298.

15. Patel, A. M., d'Avila, A., Neuzil, P., Kim, S. J., Mela, T., Singh, J. P., et al. (2008). Atrial tachycardia after ablation of persistent atrial fibrillation: identification of the critical isthmus with a combination of multielectrode activation mapping and targeted entrainment mapping. *Circulation. Arrhythmia and Electrophysiology, 1*, 14–22.
16. Dello Russo, A., Pelargonio, G., & Casella, M. (2008). New high-density mapping catheter: helpful tool to assess complete pulmonary veins isolation. *Europace, 10*, 118–119.
17. Sanders, P., Hocini, M., Jaïs, P., Hsu, L. F., Takahashi, Y., Rotter, M., et al. (2005). Characterization of focal atrial tachycardia using high-density mapping. *Journal of the American College of Cardiology, 46*, 2088–2099.
18. Beinart, R., Perna, F., Danik, S., Barrett, C. D., Heist, E. K., Ruskin, J., et al. (2010). Initial experience with a multielectrode catheter equipped with the single-axis sensor technology for high-density electroanatomical mapping in a Swine model. *Journal of Cardiovascular Electrophysiology, 21*, 1403–1407.
19. Higa, S., Tai, C. T., Lin, Y. J., Liu, T. Y., Lee, P. C., Huang, J. L., et al. (2004). Focal atrial tachycardia: new insight from noncontact mapping and catheter ablation. *Circulation, 109*, 84–91.
20. Rostock, T., Rotter, M., Sanders, P., Takahashi, Y., Jaïs, P., Hocini, M., et al. (2006). High-density activation mapping of fractionated electrograms in the atria of patients with paroxysmal atrial fibrillation. *Heart Rhythm, 3*, 27–34.
21. Reddy, V. Y., Morales, G., Ahmed, H., Neuzil, P., Dukkipati, S., Kim, S., et al. (2010). Catheter ablation of atrial fibrillation without the use of fluoroscopy. *Heart Rhythm, 7*, 1644–1653.
22. Nakagawa, H., Ikeda, A., Sharma, T., Lazzara, R., & Jackman, W. M. (2012). Rapid high resolution electroanatomic mapping. *Circulation. Arrhythmia and Electrophysiology, 5*, 417–424.
23. Zeger, S. L., & Liang, K. Y. (1986). Longitudinal data analysis for discrete and continuous outcomes. *Biometrics, 42*, 121–130.
24. Marchlinski, F. E., Callans, D. J., Gottlieb, C. D., & Zado, E. (2000). Linear ablation lesions for control of unmappable ventricular tachycardia in patients with ischemic and nonischemic cardiomyopathy. *Circulation, 101*, 1288–1296.
25. Saksena, S., Skadsberg, N. D., Rao, H. B., & Filipecki, A. (2005). Biatrial and three-dimensional mapping of spontaneous atrial arrhythmias in patients with refractory atrial fibrillation. *Journal of Cardiovascular Electrophysiology, 16*, 494–504.
26. Solheim, E., Off, M. K., Hoff, P. I., Ohm, O. J., & Chen, J. (2009). Electroanatomical mapping and radiofrequency catheter ablation of atrial tachycardia originating from the donor heart after orthotopic heart transplantation in a child. *Journal of Interventional Cardiac Electrophysiology, 25*, 73–77.
27. Verma, A., Kilicaslan, F., Schweikert, R. A., Tomassoni, G., Rossillo, A., Marrouche, N. F., et al. (2005). Short- and long-term success of substrate-based mapping and ablation of ventricular tachycardia in arrhythmogenic right ventricular dysplasia. *Circulation, 111*, 3209–3216.
28. Avella, A., d'Amati, G., Pappalardo, A., Re, F., Silenzi, P., Laurenzi, F., et al. (2008). Diagnostic value of endomyocardial biopsy guided by electroanatomic voltage mapping in arrhythmogenic right ventricular cardiomyopathy/dysplasia. *Journal of Cardiovascular Electrophysiology, 19*, 1127–1134.
29. Pieroni, M., Dello Russo, A., Marzo, F., Pelargonio, G., Casella, M., Bellocci, F., et al. (2009). High prevalence of myocarditis mimicking arrhythmogenic right ventricular cardiomyopathy differential diagnosis by electroanatomic mapping-guided endomyocardial biopsy. *Journal of the American College of Cardiology, 53*, 681–689.
30. Koruth, J. S., Heist, E. K., Danik, S., Barrett, C. D., Kabra, R., Blendea, D., et al. (2011). Accuracy of left atrial anatomical maps acquired with a multielectrode catheter during catheter ablation for atrial fibrillation. *Journal of Interventional Cardiac Electrophysiology, 32*, 45–51.

Editorial Commentary

In this study, the authors address an important clinical issue given the importance of an accurate and rapid characterization of cardiac anatomy and electrical activation for subsequent ablation. The goal is to investigate whether or not it is feasible to map the right atrium and left ventricle using a novel multielectrode catheter.